Digital and optical image from computer simulated Fresnel holograms

J.L. Juárez-Pérez[1], A. Olivares-Pérez, and L.R. Berriel-Valdos
Instituto Nacional de Astrofísica, Óptica y Electrónica, Departamento de Óptica
Apartado postal 51 and 216, 72000 Puebla, Pue., Mexico
[1]*e-mail:jjuarez@inaoep.mx*

Recibido el 12 de enero de 1996; aceptado el 18 de septiembre de 1998

Computer simulated Fresnel holograms and their numerical reconstruction are obtained in this work using binaries and gray levels images like objects. The Fresnel-Kirchhoff theory is applied without restrictions to implement the digital hologram. The same theory is taken to simulate numerically the object obtained from the digital hologram. In the optical reconstruction process from the digital Fresnel hologram a real image for either binary or gray object can be visualized with a higth quality images and low level noise.

Keywords: Digital holograms; Fresnel diffraction

En este trabajo se lleva a cabo la simulación numérica de la generación y reconstrucción de hologramas digitales de Fresnel, usando objetos bidimensionales binarios y de tonos de gris. Tanto para implementar estos hologramas digitales como para reconstruirlos numéricamente se utiliza la teoría de Fresnel-Kirchhoff sin restricciones. Al visualizar la reconstrucción óptica de estos hologramas se observa un nivel de ruido bajo y alta calidad de las imágenes.

Descriptores: Hologramas digitales; difracción de Fresnel

PACS: 42.40.J

1. Introduction

Since the appearance of the first digital hologram, a breach opened up to a new area of interest, as much academic as technological; at the date new technological applications are carried out, using holograms generated by computer (HGC) [1, 2]. From a beginning the decoding technique of digital holograms has been their binarization and even some authors continue employing it [3, 4]. Above this, they have proposed many binarization techniques with the goal of reducing the noise in which the image reconstructed is involves [4–7]. On the other hand, the use of the technique of fast Fourier transform (FFT) have been employed, for their low cost computer, for the obtaining of the near and distant diffraction field [8, 9]. Some works are supported by the angular spectrum theory [10–12], that represent in the frequency space the Fresnel-Kirchhoff formula, with this way wend is applied the FFT algorithm, is very fast to make the hologram. However exist a strong restriction, this restriction is due by the point numbers contained in the object, because in the frequencial space the number of elements are equal to the size elements from the object [13], with this limitation, in the reconstruction step the image has low quality.

Up day the Fresnel-Kirchhoff theory has a new impetus [14–16] because the new computer machine open the possibility to obtain these holograms with this way to represent more exactly possible the holographic field as their reconstruction too.

In this work is applied without restriction the Fresnel-Kirchhoff scalar diffraction theory without the use of the FFT is implemented, with the purpose of obtaining the diffraction field the most accurate possible. The results are shown applied to flat objects with levels of gray and binary. The direct fotoreduction of the HGC, visualized in a computer monitor, is obtained; this way the representation of the HGC is nearer to the reality to difference of their binary representation. In the reconstructed with light laser, the holographic images presenting a low level of noise and focused, so much the real and conjugated image, in several planes of depth.

2. Theory

The intensity distribution pattern produced by the interference fringes in the holographic plate due to the superposition of the two wave fronts is given by

$$E(x,y) = |O(x,y) + R(x,y)|^2, \tag{1}$$

where $O(x,y)$ and $R(x,y)$ are the complex amplitude distribution functions associated to the object and to the reference wave front respectively. Because the process of wave front propagation from the object plane to the holographic plate can be obtained from the Fresnel-Kirchhoff diffraction formula, the object wave front distribution function at the holographic plane may be represented by [9]

$$O(x,y) = \int_{-\alpha}^{\alpha}\int_{-\alpha}^{\alpha} \frac{I(X,Y)e^{jkr}\cos(\vec{n}\cdot\vec{r})}{r}\,dX\,dY, \tag{2}$$

where $I(X,Y)$ is the complex amplitude function of the object in the object plane, $k = 2\pi/\lambda$ is the wave number, λ is the wave length used in the reconstruction step, and

$r = [(x-X)^2 + (y-Y)^2 + s^2]^{1/2}$ is the distance between any point in the object plane (X, Y) and any point in the hologram plane (x, y), $\cos(\vec{n} \cdot \vec{r})$ is the obliquity factor. Because the object is discrete we work with digital images, and Eq. (2) takes the form

$$O(x_l, y_m) = \sum_{q=0}^{Q-1} \sum_{p=0}^{P-1} \frac{I(X_p, Y_q)}{r_{p,q}^{l,m}} e^{jkr_{p,q}^{l,m}}, \qquad \begin{matrix} l = 0, \ldots, L-1, \\ m = 0, \ldots, M-1, \end{matrix} \tag{3}$$

where l, m, p and q are real integer numbers. The indices l, m are the number of elements in the hologram matricial array in the holographic plane, the indices p, q correspond to the number of elements in the object matricial array. The values of P and Q indicate the total number of object-samples in the x and y directions, similarly, the L and M values indicate the total number of samples in the X and Y directions at the hologram plane. All the possible values for $r_{p,q}^{l,m}$ are given by the relationship

$$r_{p,q}^{l,m} = \sqrt{(X_p - x_l)^2 + (Y_q - y_m)^2 + s^2}, \qquad \begin{matrix} l = 0, \ldots, L-1, \\ m = 0, \ldots, M-1, \\ p = 0, \ldots, P-1, \\ q = 0, \ldots, Q-1. \end{matrix} \tag{4}$$

which is the radius of the divergen spherical waves which emerges from the object and arrive to the holographic plane. The function $O(x_l, y_m)$ represents the discrete wave front that is detected in the holographic plane.

3. Reference plane wave

If the reference plane wave has some tilt, then

$$R(x_l, y_m) = Ae^{j\vec{k}\cdot\vec{r}l,m}, \quad \begin{matrix} l = 0, \ldots, L-1; \\ m = 0, \ldots, M-1. \end{matrix} \tag{5}$$

where the wave number vector, $\vec{k}$, is represent by

$$\vec{k} = \frac{2\pi}{\lambda}[\cos(\theta_x)\hat{\imath} + \cos(\theta_y)\hat{\jmath} + \cos(\theta_z)\hat{k}], \tag{6}$$

and $\cos(\theta_x)$, $\cos(\theta_y)$, $\cos(\theta_z)$ and $\hat{\imath}, \hat{\jmath}, \hat{k}$ are the director cosines and the normalized vector in the x, y and z directions, respectively. The distance vector $\vec{r}_{lm}$ has the following relation with the x_l, y_m and s values:

$$\vec{r}_{l,m} = x_l\hat{\imath} + y_m\hat{\jmath} + s\hat{k}, \quad \begin{matrix} l = 0, \ldots, L-1; \\ m = 0, \ldots, M-1. \end{matrix} \tag{7}$$

Because we want fringes in the digital hologram with maximum visibility value, one possible way to choose the amplitude value of reference wave, A, is given by

$$A = \left| \sum_{q=0}^{Q-1} \sum_{p=0}^{P-1} \frac{I(X_p, Y_q)}{r_{p,q}^{l,m}} e^{jkr_{p,q}^{l,m}} \right| \tag{8}$$

4. Digital hologram record

The complex amplitude at each hologram cell $H(x_l, y_m)$ in the holographic plane can be calculated adding Eqs. (3) and (5):

$$H(x_1, y_m) = Ae^{j\vec{k}\cdot\vec{r}_{l,m}} + \sum_{q=0}^{Q-1} \sum_{p=0}^{P-1} \frac{I(X_p, Y_q)}{r_{p,q}^{l,m}} e^{jkr_{p,q}^{l,m}}, \qquad \begin{matrix} l = 0, \ldots, L-1, \\ m = 0, \ldots, M-1, \\ p = 0, \ldots, P-1, \\ q = 0, \ldots, Q-1. \end{matrix} \tag{9}$$

and the irradiance distribution, $E(x_l, y_m)$, is the product of $H(x_l, y_m)$ with its complex conjugate, therefore we obtain

$$E(x_l, y_m) = |A|^2 + \sum_{q=0}^{Q-1} \sum_{p=0}^{P-1} \left| \frac{I(X_p, Y_q)}{r_{p,q}^{l,m}} \right|^2 + 2 \sum_{\substack{q'=0 \\ q' \neq q}}^{Q-2} \sum_{q=1}^{Q-1} \sum_{\substack{p'=0 \\ p' \neq p}}^{P-2} \sum_{p=1}^{P-1} \frac{I(X_p, Y_q)}{r_{p,q}^{l,m} r_{p',q'}^{l,m}} \cos\left[k\left(r_{p',q'}^{l,m} - r_{p,q}^{l,m}\right)\right] + 2A \sum_{q=0}^{Q-1} \sum_{p=0}^{P-1} \frac{I(X_p, Y_q)}{r_{p,q}^{l,m}} \cos\left(\vec{k}\cdot\vec{r}_{l,m} - kr_{p,q}^{l,m}\right), \qquad \begin{matrix} l = 0, \ldots, L-1, \\ m = 0, \ldots, M-1, \end{matrix} \tag{10}$$

Equation (10) indicates that the irradiance value in each cell in the holographic plane is the contribution of a constant value due to the first term. The other three terms are inversely proportional to the distance between the objet cells and the hologram cells coordinates. Also, the second term depends directly of the irradiance value associated to each object cell and the third term is determined by the reference value between the emergent spherical wave of each two different cells from the object. Finally, the fourth term is the contribution of all the diverging spherical wave fronts coming out from the object cells with the reference wave front.

5. Useful parameters

The numerical implementation of Eq. (10) involves the assignation of some parameters values, for example: the resolution and physical sizes in both the objet and digital hologram plane, the distance between the object and the hologram planes and the amplitude and tilt of the reference wave. Some of these parameters are related and some can be choose.

The resolution of the digital hologram can be obtained from the grating equation, which is given by

$$d \cdot \sin(\phi) = n \cdot \lambda \qquad (n = 0 \pm 1), \tag{11}$$

where d is the fringe period values, ϕ is the angle between the objet and reference wavefront and n is the diffraction order

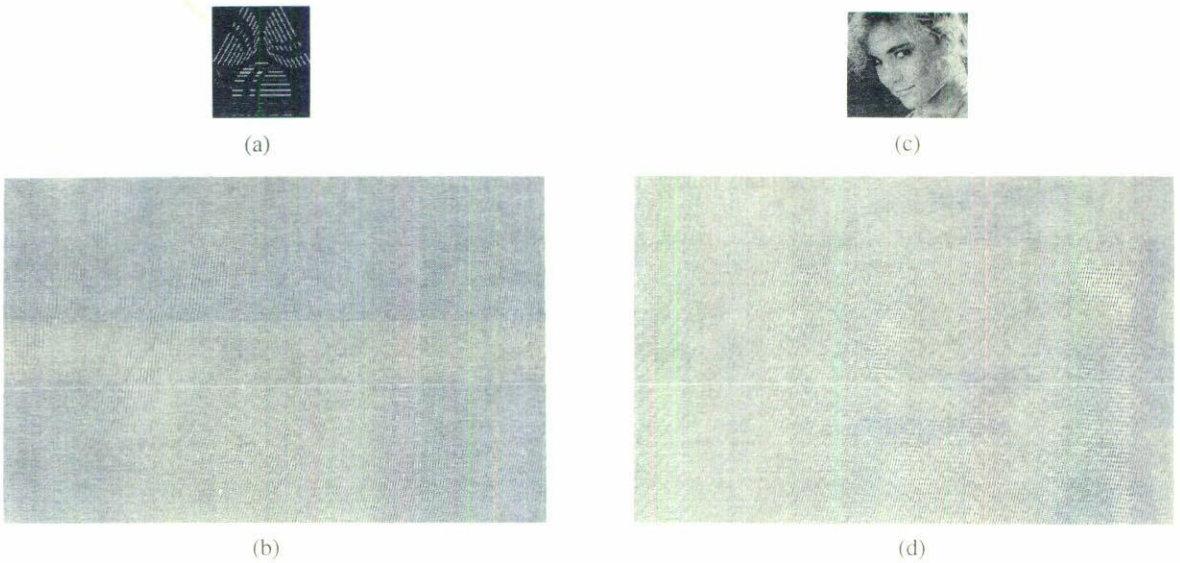

FIGURE 1. a) Correspond to a binary image employed to make the hologram. It is represented by a matricial array of 330 × 378 pixels. b) Is the hologram of the binary image. Here it is possible to see that this hologram is not binary, and has 64 gray levels. This hologram corresponds to a matricial array of 500 × 500 pixels. c) Correspond to a image with gray levels, it is represented by a matricial array of 100 × 100 pixels, that is used to make the hologram. d) Is its hologram with the same conditions as (b)

number. This resolution can be calculated when the interference pattern fringes have a minimum period value, $d_{\min}$, which is obtained using the reference wave with the most distant point of the objet, this minimum period value is given by

$$d_{\min} = \frac{\lambda}{\sin(\phi_{\max})}, \tag{12}$$

where

$$\phi_{\max} = \max\{\sin^{-1}\left(\frac{\bar{k}\cdot\bar{r}_{p,q}^{l,m}}{|\bar{k}|\cdot|\bar{r}_{p,q}^{l,m}|}\right)\} \tag{13}$$

is the maximum angle between the vectors $\bar{k}$, and $\bar{r}_{p,q}^{l,m}$. Therefore if we know the minimum period, the hologram resolution in the x and y directions is determined by the maximum frequency or by the number of the minimum period period per unit of length $f_{\max}$, this implies that the maximum frequency is

$$f_{\max} = \frac{1}{d_{\min}}. \tag{14}$$

6. Results

The binary object and the gray level object used to make the digital hologram are shown in Fig. 1a and Fig. 1c, respectively. This digital hologram was numerically calculated and has sixty four gray levels with 768 by 768 pixels. The computer time wasted away in the hologram simulating was about 126 hr. of CPU, using a 486-66 Personal Computer, Fig. 1b and Fig. 1d. In order to record photographically more information from the weak fringes of the interference pattern, it was necessary to display logaritmically the digital hologram on the monitor screen (using the following relation: $\log[1 + E(x_l, y_m)]$). To obtain the transmittance function of the physical hologram a photography of the VGA monitor was taken. The physical size of the image in the screen is 17 cm by 17 cm and the Screen resolution is 1024 by 768 pixels. We reduced it photographically such that the real size of the digital hologram is 2 cm by 2 cm. A Nikon FM2 camera with the holographic film SO-253 were used in the photograph and reducing step.

The optical reconstruction of the digital Fresnel hologram was carried out with the set up shown in Fig. 2. In this case the image was reconstructed taking in to account the same distance to the original position of the object. As we can observe Fig. 3a shows three images that were obtained with optical reconstruction, the zero order, the diffraction pattern of the image conjugate pseudoscopic, and the real orthoscopic image. Figure 3b This scene shows the simulated reconstruction and it is possible to see the whole field with all kind of details formed by the zero order and the two first diffracted orders. Figure 4a shows four images obtained in the optical reconstruction, the zero order, the diffraction pattern of the image conjugate pseudoscopic, and the real orthoscopic image, the other two dark images correspond to higher orders. Figure 4b shows the simulated reconstruction and it is possible to see the whole field with all kinds of details formed by the zero order and the two first diffracted orders, as its higher orders. reconstruction, the zero order, the diffraction pattern of the image conjugate pseudoscopic, and the real orthoscopic image, the other two dark images correspond to higher orders. Figure 4b shows the simulated reconstruction and it is possible to see the whole field with all kinds of details formed by the zero order and the two first diffracted orders, as its higher orders.

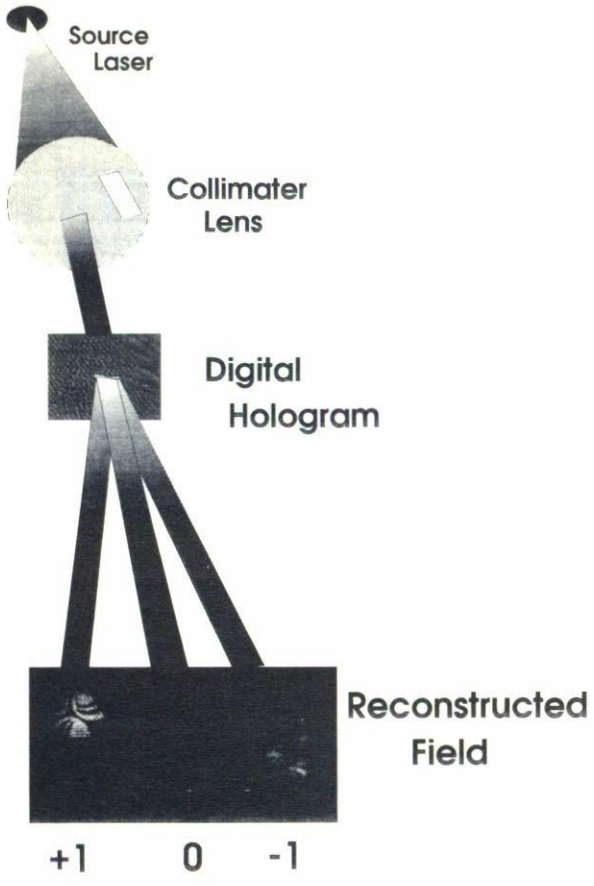

FIGURE 2. Setup employed for the optical reconstruction of the digital Fresnel hologram.

7. Conclusions

In this work we made the digital and optical reconstruction of digital Fresnel hologram using the Fresnel-Kirchhoff theory with the intention of the have the most exact possible the diffraction fields. These Fresnel holograms was recorded in different gray tones. The big difference between Diffraction Fresnel theory using FFT is that the holographic images real and conjugate are in one plane, without FFT are in different planes; we obtained the second ones. Likewise the reconstructed holographic real images have similar amplification and distance than the original object. We obtained holographic image with a signal to noise ratio better than those reports using FFT.

Acknowledgments

J.L. Juarez-Perez is supported by a fellowship from Consejo Nacional de Ciencia y Tecnología (CONACyT).

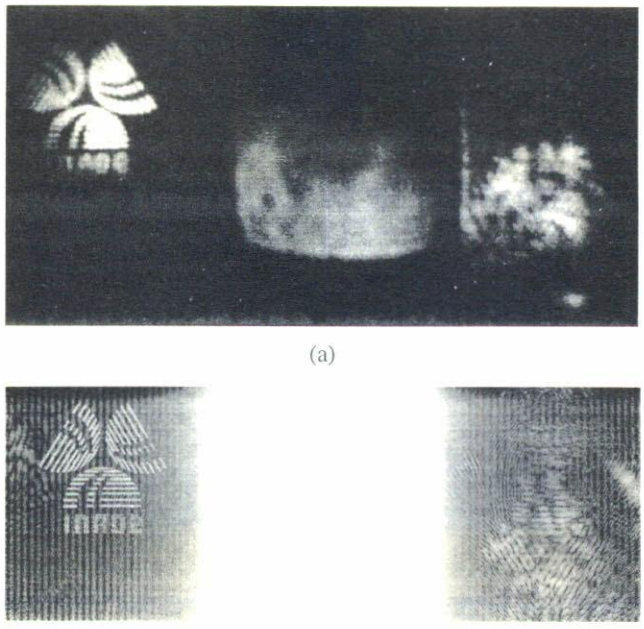

(a)

(b)

FIGURE 3. a) This photograph represents the binary object. In the optical reconstruction of the field, we observe the real orthoscopic image, zero order, and the diffraction pattern of the conjugate real pseudoscopic image. b) Shows the image obtained in the simulated numerical reconstruction.

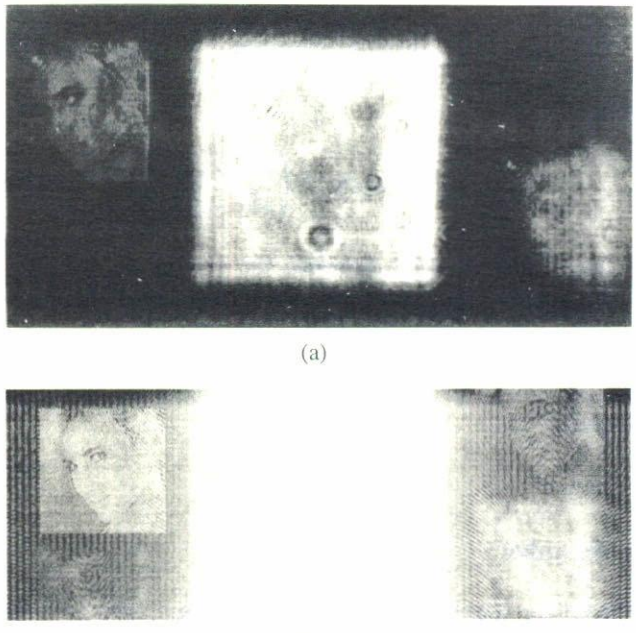

(a)

(b)

FIGURE 4. a) This photograph represent the 64 levels gray object, the optical reconstructing of the field, where are localized the real orthoscopic image, zero order, and the diffraction pattern of the conjugate real pseudoscopic image. b) Shows the image obtained in the simulated numerical reconstruction.

1. B.R. Brown and A.W. Lohmann, *Appl. Opt.* **5** (1966) 967.
2. A.W. Lohmann and D.P. Paris, *Appl. Opt.* **6** (1967) 1739.
3. B.R. Brown and A.W. Lohmann, *IBM J. Res. Develop.* **13** (1969) 160.
4. J.A. Hudson, *Appl. Opt.* **23** (1984), 2292.
5. C.D. Carey *et al. Electron. Lett.* (1992) 2082.
6. S.H. Song *et al. Appl. Opt.* **99** (1993) 5022.
7. R. Ecshbach, *Appl. Opt.* **30** (1991) 3702.
8. Chien-Hsien Wu, Chia-Lun Chen, and M.A. Fiddy, *Appl. Opt.* **32** (1993) 5135.
9. H.J. Caulfield, *Handbook of Optical Holography*, (Academic Press, New York, 1979).
10. H. Osterberg, *JOSA* **55** (1965) 1467.
11. G.C. Sherman, *JOSA* **57** (1967) 546.
12. R.J. Collier, C.B. Burchhardt, and L.H. Lin, *Optical Holography*, (Academic Press, New York,1971).
13. R.N. Bracewell, *The Fourier Transform and its Application*, (Mc Graw-HillBook Company, New York, 1978).
14. M. Lucente, *Journal of Elec. Imag.* **2** (1993) 1.
15. M. Lucente, *Opt. Eng.* **35** (1996) 1529.
16. M. Lucente, *IBM Syst.* **35** (1996) 3.